CrossMark

Study of nickel catalysts for hydrogen production in sorption enhanced reforming process

Ana L. García-Lario*, María Aznar, Gemma S. Grasa, Tomás García, Ramón Murillo

Environmental Research Group, Instituto de Carboquímica, CSIC, C/Miguel Luesma Castán 4, E-50018 Zaragoza, Spain

HIGHLIGHTS

- Ni based catalysts were compared to be used in sorption enhanced reforming.
- NiO/Si_3N_4 showed low CH_4 conversion at sorption enhanced reforming temperature.
- 10% $NiO/NiAl_2O_4$ and 20% $NiO/\alpha-Al_2O_3$ are suitable to be applied in SER.
- The observed trend of carbon formation over catalysts was $Si_3N_4 > Al_2O_3 > NiAl_2O_4$.

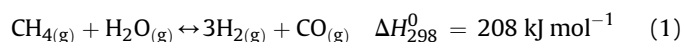## ARTICLE INFO

ABSTRACT

The performance of Ni based catalysts to be used in Sorption Enhanced Reforming (SER) is assessed. For this aim, both their activity at low temperature and their behavior during multiple oxidation–reduction cycles in steam methane reforming are studied. Ni catalysts supported on $\alpha-Al_2O_3$, Si_3N_4 and $NiAl_2O_4$, with different amounts of Ni (0–50% NiO), are compared by testing their activity in a fixed bed micro-reactor. While Ni/Si_3N_4 catalysts do not show an appropriate performance at low temperature, $Ni/\alpha-Al_2O_3$ and $Ni/NiAl_2O_4$ present a significant activity, close to equilibrium data, at the typical SER conditions. The best experimental results are attained for 20% $NiO/\alpha-Al_2O_3$ and 10% $NiO/NiAl_2O_4$ catalysts that show an activity close to the equilibrium for steam to methane ratio of 4.5. Higher amounts of NiO in both catalysts do not reveal an improvement in conversion results. In addition, both 20% $NiO/\alpha-Al_2O_3$ and 10% $NiO/NiAl_2O_4$ catalysts show a good reforming activity after oxidation–reduction cycles at typical SER temperatures. The observed trend to carbon deposition on the catalyst surface for the studied supports is $Si_3N_4 > Al_2O_3 > NiAl_2O_4$, being negligible when $NiAl_2O_4$ support is used. These results suggested that 10% $NiO/NiAl_2O_4$ and 20% NiO/Al_2O_3 catalysts could be perfect candidates to be used in SER process.
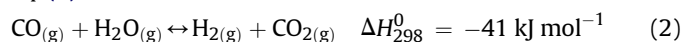
© 2013 Elsevier B.V. All rights reserved.

1. Introduction

It is well known that hydrogen is an advantageous energy carrier due to its clean combustion products and easy conversion to generate heat or electricity [1]. In addition, hydrogen is used as a feedstock in many industrial processes such as petroleum refining, ammonia or methanol production [2]. Therefore an increasing demand of hydrogen is expected in the short term. Most of the hydrogen produced worldwide is obtained from natural gas conversion. However, the possible depletion of gas fields together with an increase in global warming, make necessary to develop new

efficient processes with low CO_2 emissions. Nowadays, steam reforming of natural gas is the most economical and widely used technology for H_2 production in industrial applications [1,3–6]. This process includes several steps in pressure and temperature under severe conditions. The first step is the reforming of methane with steam at 800–900 °C and 15–30 bar in tubular reactors externally heated and filled with nickel based catalyst, mainly producing H_2 and CO according to Eq. (1):

$$CH_{4(g)} + H_2O_{(g)} \leftrightarrow 3H_{2(g)} + CO_{(g)} \quad \Delta H^0_{298} = 208 \text{ kJ mol}^{-1} \quad (1)$$
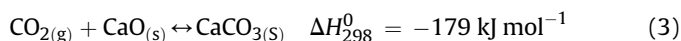
The next step in this process is the water gas shift reaction (WGS) (high and low temperature stages) where undesired CO is converted to CO_2 and hydrogen yield is increased according to Eq. (2):

$$CO_{(g)} + H_2O_{(g)} \leftrightarrow H_{2(g)} + CO_{2(g)} \quad \Delta H^0_{298} = -41 \text{ kJ mol}^{-1} \quad (2)$$
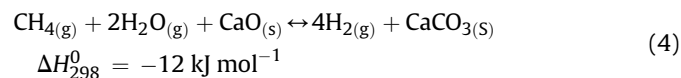
* Corresponding author. Tel.: +34 976 7733977; fax: +34 976 733318.
E-mail addresses: algarcia@icb.csic.es (A.L. García-Lario), m.aznar@icb.csic.es (M. Aznar), gga@icb.csic.es (G.S. Grasa), tomas@icb.csic.es (T. García), ramon.murillo@icb.csic.es (R. Murillo).

At last, optional purification methods, like pressure swing adsorption, allow high H_2 concentrations in the final product [3,4,7]. Although steam reforming is the dominant process for commercial hydrogen production, it is very energy intensive and high CO_2 producer [3]. So, it is necessary to develop new commercial technologies in order to improve that process, such as Sorption Enhanced Reforming (SER). In this process, the reforming catalyst is combined with a CO_2 acceptor (a sorbent, usually based on CaO) in order to in situ remove the CO_2 as soon as it is formed (Eq. (3)):

$$CO_{2(g)} + CaO_{(s)} \leftrightarrow CaCO_{3(S)} \quad \Delta H^0_{298} = -179 \, \text{kJ mol}^{-1} \tag{3}$$

Thus, all steps (reforming, WGS and CO_2 removal) take place in the same reactor [4] with the total reaction given in Eq. (4):

$$CH_{4(g)} + 2H_2O_{(g)} + CaO_{(s)} \leftrightarrow 4H_{2(g)} + CaCO_{3(S)}$$
$$\Delta H^0_{298} = -12 \, \text{kJ mol}^{-1} \tag{4}$$

The sorbent addition makes the overall process slightly exothermic and shifts the equilibrium to favor the formation of higher hydrogen concentrations. Potential benefits from the SER process are extensively reported in the literature, such as lower operational temperatures (600 °C–700 °C), CO_2 capture, and the production of high purity H_2 [4], making this process attractive compared to the traditional steam reforming process that operates at industrial scale.

In a commercial process, the sorbent must be regenerated by calcination of $CaCO_3$ to CO_2 in an additional step to be reused, so a cyclic system consisting of two interconnected fluidized-bed reactors (reforming reactor and calcination reactor) has been proposed [7–10]. This technology allows to remove the spent sorbent and add fresh one during the process in order to get a continuously regenerated sorbent flow transferred to the reforming reactor. A conceptual scheme is shown in Fig. 1:

Reforming, WGS and carbonation reactions take place in the reforming reactor where a mixture of catalyst and sorbent is present. This reactor operates at low temperature ($\approx$ 600 °C–700 °C) and atmospheric pressure, resulting in a high purity H_2 stream, with steam and low quantities of CO, CO_2 and CH_4.

In the second reactor (calcination–oxidation) the used mixture of catalyst and spent sorbent is submitted to high temperature (depending on CO_2 partial pressure) to regenerate the sorbent. Additional fuel is required to provide the necessary heat to this

step. O_2 is also added with this fuel to obtain a gas stream with concentrated CO_2.

The solid mixture of sorbent and catalyst is circulating continuously between the two beds, being repeatedly exposed to different reaction environments (oxidation–reduction) by short time intervals. The use of different sorbents in the SER process has been widely studied in the literature [4,11]. However, it is also necessary to find and to study appropriate reforming catalysts able to work at typical SER temperatures and in multiple cyclic operation (oxidation–reduction cycles). In addition, these catalysts must also be able to operate, if possible, at low steam/methane ratios in order to improve the energy efficiency of the process.

Ni has been generally used as the catalyst in steam methane reforming (SMR) because it presents a high activity and has a lower cost than other precious metals [3]. α-Al_2O_3 is frequently used as support due to its stability at high temperatures, lower trend to $NiAl_2O_4$ formation than γ-Al_2O_3, and its low price [3,12]. However, it is well known that this catalyst shows deactivation problems due to carbon formation during SMR [12–16]. Up to now, the catalytic activity of 15–20% NiO/α-Al_2O_3 has been studied in SER process at atmospheric pressure in a fixed bed reactor, showing satisfactory results with respect to methane conversion and hydrogen production [7,17–19].

Other promising catalysts could be NiO/Si_3N_4 and NiO/$NiAl_2O_4$ that have been used in other processes and, according to the literature, have good properties regarding to low catalyst coking and cyclic operation capacity [20,21].

Ni/Si_3N_4 has been used at high temperatures in the partial oxidation of methane to produce syngas. The results reported in the literature show that Si_3N_4 supported nickel catalyst have good catalytic activity and resistance to coke formation, mainly due to the interaction between the metal and the basic support [22].

Ni/$NiAl_2O_4$ catalyst has been used in several fields due to its resistance to high temperature and acidic or basic environments [23]. It has been applied in chemical looping showing good cyclic performance [20,24]. The good catalytic activity of this material has been also reported for SMR [6]. In addition, there are few studies applying this catalytic system in SER process but always at very high Ni contents [10,25].

In this scenario, the aim of the present work is to compare the catalytic activity in methane steam reforming of α-Al_2O_3, Si_3N_4 and $NiAl_2O_4$ supports with different NiO charges in order to select the most appropriate catalysts to be implemented in SER process. To achieve this objective, catalysts with diverse NiO loadings have
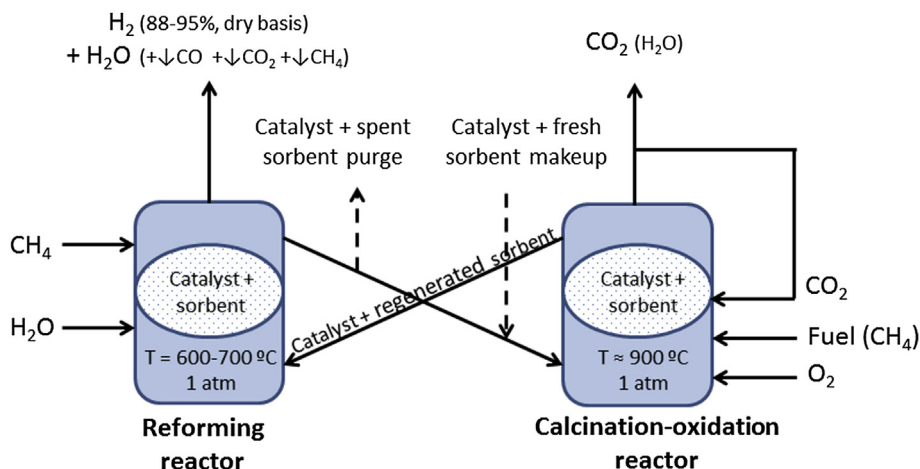

Fig. 1. Sorption enhanced process conceptual scheme.

been synthesized and characterized. Their catalytic activity has been evaluated in a fixed bed micro-reactor according to typical SER temperatures. The most active catalysts have been also tested after successive oxidation–reduction cycles. Finally, the influence of steam to methane ratio (S/C), activity with time and space velocity has been assessed for NiO/NiAl$_2$O$_4$.

2. Experimental

2.1. Catalysts synthesis

The supports used in this study included commercial Si$_3$N$_4$ (Sigma Aldrich, $S_{BET} = 11$ m^2 g^{-1}), and α-Al$_2$O$_3$ ($S_{BET} = 15$ m^2 g^{-1}), which was prepared by calcining commercial γ-Al$_2$O$_3$ (Puralox NWa-155) at 1150 °C for 3 h. These catalysts were prepared by impregnation of that supports with Ni(NO$_3$)$_3$·6H$_2$O (>97% from Sigma Aldrich) aqueous solution to reach a final NiO content of 10–20–40 wt.%. After drying at 80 °C overnight, the samples were calcined in air flow at 400 °C for 4 h. Finally the catalysts were calcined at 900 °C for 1 h.

In addition, NiO/NiAl$_2$O$_4$ catalysts were prepared following the description of Readman et al. [24]. Appropriate amounts of Al(NO$_3$)$_3$·9H$_2$O (>98.5 from Sigma Aldrich) and Ni(NO$_3$)$_2$·6H$_2$O (>97% from Sigma Aldrich) were dissolved separately in a solvent which is 50/50 mix of 2-propanol and water. Once dissolved, the two solutions were mixed together to reach a final NiO content of 5–10–20–50 wt.%. The resulting solution was stirred and heated at 230 °C until the desired viscosity was obtained. The mixture was then dried in an oven at 150 °C for two days. The dry product was crushed by a mortar and, finally, the obtained powder was calcined in air at 1200 °C for 6 h (heating rate of 5 °C min^{-1}). In all cases, the final powder was crushed and sieved (100–200 μm).

2.2. Catalysts characterization

Several techniques were used for textural, chemical and structural characterization of catalysts. The BET areas of the catalysts were determined by nitrogen adsorption at −196 °C in a Micromeritics ASAP-2020. Crystalline phases and mean crystallite sizes were carried out by XRD analysis in an X-ray diffractometer Bruker AXS D8ADVANCE using the Cu Kα radiation. In order to check the amount of active nickel in each catalyst, reduction tests were performed in a thermo-gravimetric analyzer (TGA), described elsewhere by Garcia-Lario et al. [26]. The reduction temperature from free NiO to metallic nickel for the studied supports is reported in the literature [6,21,27]. So, each sample was heated in a 10% vol. H$_2$/N$_2$ flow at 650 °C, which is an appropriate temperature to avoid the undesired reduction of NiAl$_2$O$_4$ [6]. In this way, the loss of weight was only due to NiO reduction. Scanning electron microscopy (SEM) using a Hitachi S-3400 N was applied in order to determine the morphology of the samples. In addition, energy dispersive X-ray (EDX) analysis was used to evaluate the nickel distribution. The carbon deposition of fresh and used catalyst was also determined by EDX.

2.3. Catalytic activity measurement

Experiments were carried out in the fixed bed micro-reactor shown in Fig. 2. The experimental system allowed feeding CH$_4$, N$_2$ and H$_2$ by means of the corresponding mass flow controllers. Water was fed using a pressurized vessel and a mass flow controller. The water flow was evaporated in a stainless steel pipe heated at 200 °C by a cylindrical electric furnace connected to a temperature controller. Steam was then mixed with the N$_2$ and CH$_4$ flows before entering to the steam reforming reactor.

Reforming experiments were conducted in a 250 mm length tubular quartz reactor, with an inner diameter of 6 mm in the upper
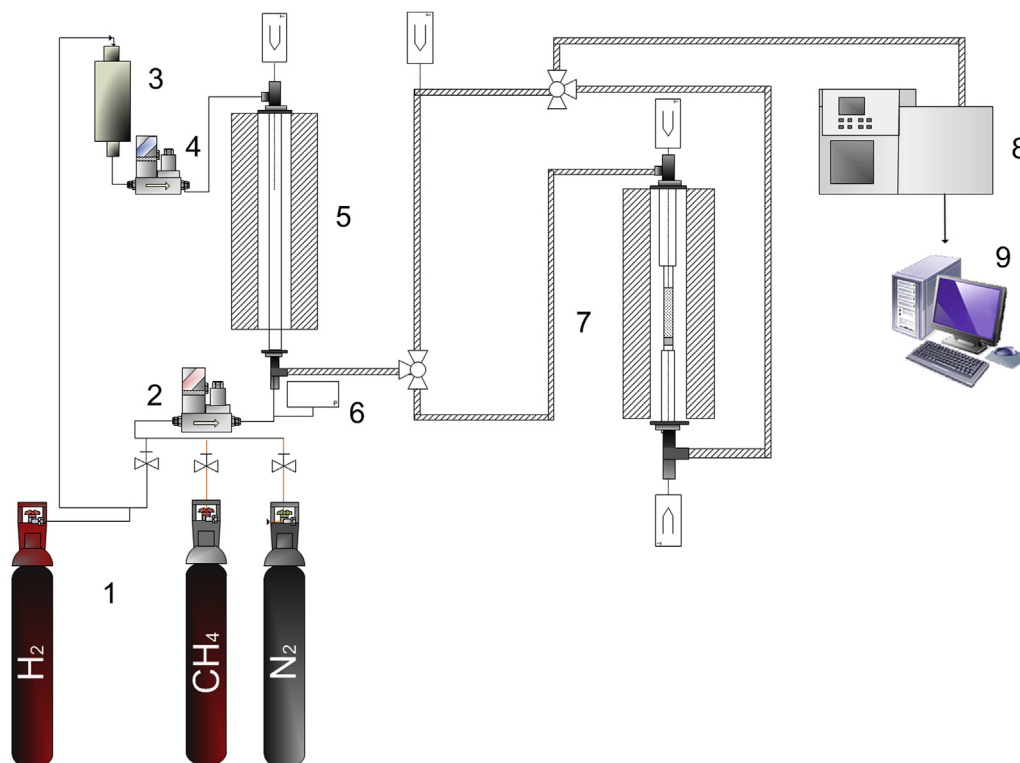

Fig. 2. Fixed bed reactor system. (1: CH$_4$, N$_2$ and H$_2$; 2: gas mass flow controllers; 3: water pressurized vessel; 4: liquid mass flow controller; 5: evaporator; 6: manometer; 7: fixed bed; 8: gas chromatograph; 9: data acquisition system).

and bottom sections, and 4 mm in the middle part, where the catalyst was placed on a fritted quartz disc. The reactor was placed inside a cylindrical electrically heated oven. Two thermocouples were used to measure the temperature in the fixed bed: the first one was used to control the process temperature and was touching the upper section of the catalyst bed, and the second one was below the fritted disk. After the reactor, a recovery system to condensate water was disposed. Finally, the gas composition was determined by means of a gas chromatograph (Varian CP-3800) online fitted to the process. N_2 was used as an internal standard to quantify the outside gas production.

Firstly, the catalytic activity of different NiO loadings (10–50 wt.%) on three different supports (α-Al_2O_3, $NiAl_2O_4$ and Si_3N_4) was tested at 400 °C–785 °C, a steam to methane ratio of 4.5, and a space velocity for CH_4 of 4000 h^{-1}. A bed of approximately 40 mm was used in the experiments performed. The calculated dispersion coefficient was low in order to assure plug-flow throughout the reactor [28]. Before each reaction tests, the catalysts were in situ reduced at 600 °C in a 40% H_2 flow for 1 h. Besides, the Ni/$NiAl_2O_4$ catalyst was selected to perform some additional tests at lower NiO loadings (0 and 5%wt.). The experimental test duration was approximately 1 h.

As the final aim was selecting a catalyst for working in the SER process, it was also necessary to prove the activity of the catalyst after several oxidation–reduction cycles. To achieve this, the catalysts which presented the highest activity were subjected to approximately fifty oxidation/reduction cycles in the thermobalance system described elsewhere by Garcia-Lario et al. [26]. After cycling, their catalytic activities were also evaluated on the fixed bed micro-reactor at S/C = 4.5 and typical SER operation temperatures (600 °C–700 °C).

An additional parametric study was performed using 10% NiO/$NiAl_2O_4$. First, its long term activity (7 h) was tested. The steam/methane ratio influence on methane conversion was also analyzed (S/C = 2–4.5). Finally, the space velocity effect (8000 h^{-1}, 16,000 h^{-1} and 20,000 h^{-1} for CH_4) on gas composition was studied, using in this case a shorter bed (15 mm). The experimental test duration was approximately 1 h.

Table 1 shows a summary of the operating conditions for the whole set of experiments performed.

Table 1
Summary of operating conditions for the experiments.

% NiO	T (°C)	SV (CH_4) (h^{-1})	S/C	Observations
NiO/Al_2O_3				
10	400–785	4000	4.5	
20	400–785	4000	4.5	
40	400–785	4000	4.5	
20	600–700	4000	4.5	Cycled catalyst
NiO/Si_3N_4				
10	400–785	4000	4.5	
20	400–785	4000	4.5	
40	400–785	4000	4.5	
NiO/$NiAl_2O_4$				
0	600–700	4000	4.5	
5	400–785	4000	4.5	
10	400–785	4000	4.5	
20	400–785	4000	4.5	
50	400–785	4000	4.5	
10	600–700	4000	4.5	Cycled catalyst
10	600–700	4000	2.2	
10	600–700	4000	3.3	
10	650	4000	3.3	7 h
10	650	8000	4.5	
10	650	16,000	4.5	
10	650	20,000	4.5	

The experimental results from catalytic activity tests in terms of methane conversion and gas composition have been compared with the corresponding equilibrium data, calculated using the process simulator Aspen Hysys®.

3. Results and discussion

3.1. Catalyst characterization

In this section characterization results from the different synthesized catalysts are presented. Table 2 summarizes the properties of the catalysts prepared (BET surface area, NiO particle size and crystal phase in fresh catalyst). The characterization of the catalysts after experimentation will be exposed and discussed later, with the results of the different tests performed (Section 3.2).

3.1.1. BET surface area
Table 2 shows that the BET surface area of α-Al_2O_3 and Si_3N_4 supports slightly decrease with the increase of NiO loading due to the impregnation process. In these cases, BET area results are consistent with literature [21,27,29]. $NiAl_2O_4$ catalysts have lower BET surface area than Al_2O_3 and Si_3N_4 catalysts, regardless the amount of NiO supported, probably due to the method used for preparation which includes a final calcination step at high temperature (1200 °C during 6 h). The independence between NiO amount and BET surface area for NiO/$NiAl_2O_4$ catalyst has been reported in some works [6]. In addition, $NiAl_2O_4$ surface area values are in accordance with previously reported data obtained in similar synthesis route [24].

3.1.2. XRD
XRD patterns points out that no intermediate phases in $NiAl_2O_4$ and Si_3N_4 fresh catalyst are observed (see Table 2). As expected, Si_3N_4 support is stable and no nickel silicides are produced after impregnation and calcination. Likewise, nickel supported $NiAl_2O_4$ catalysts only include NiO phase [6,24]. However, α-Al_2O_3 fresh catalysts do not only show NiO and α-Al_2O_3 peaks, but also those corresponding to $NiAl_2O_4$ (Table 2). The formation of the spinel phase in nickel supported α-Al_2O_3 catalysts could be likely due to a strong nickel-support interaction at high calcination temperature [30,31]. It is interesting to point out that the spinel phase is not an active phase for methane reforming [12] being the $NiAl_2O_4$ formation a possible cause of deactivation of NiO/α-Al_2O_3 catalysts [32].

It is worth highlighting that nickel particle size is an important factor as it is well-known that small NiO particle size improves the catalyst activity and leads to catalysts more resistant to carbon formation [3,33]. Thus, crystallite mean sizes of fresh catalysts calculated from XRD profiles are shown in Table 2. As expected, it is observed for Al_2O_3 and Si_3N_4 supports that the higher the nickel loading, the larger the NiO crystallite mean size. In addition, Table 2

Table 2
Properties of the catalysts.

Support	NiO loading (%)	S_{BET} (m^2 g^{-1})	NiO particle size	Crystal phase
α-Al_2O_3	10	20.9	9.2	In all cases: Al_2O_3
	20	20.7	32.0	NiO
	40	17.7	50.2	$NiAl_2O_4$
$NiAl_2O_4$	10	1.4	112.3	In all cases:
	20	5.9	69.5	NiO
	50	3.4	85.3	$NiAl_2O_4$
Si_3N_4	10	12.3	38.3	In all cases:
	20	10.2	49.8	NiO
	40	7.5	56.5	Si_3N_4

shows that NiO crystallite mean size for both Si_3N_4 and Al_2O_3 catalysts are much lower than those found in $NiAl_2O_4$ supports, which have the lowest surface area. Finally, NiO crystallite size in $NiAl_2O_4$ supports do not follow the expected tendency with NiO loading.

3.1.3. Catalyst morphology, Ni distribution and active amount

The SEM and EDX analyses carried out to the samples show a good Ni distribution over all supports (see Supporting information). However, although Si_3N_4 and Al_2O_3 structure hardly change when NiO amount is increased (see Supporting information), $NiAl_2O_4$ structure changes are more appreciably with the NiO loading on the support. As can be seen in Fig. 3a, spinel system (0% NiO) shows a compact and smooth structure which is in concordance with literature [6]. When NiO amount increases, the samples have a more granular aspect as it is shown in Fig. 3c and d.

The amount of experimental active NiO presented in the catalysts are in agreement with theoretical NiO loadings (reported on Table 2) even for α-Al_2O_3 support, where the formation of a marginal amount of $NiAl_2O_4$ is observed. It is important to quantify the amount of free NiO due to the fact that the reduced metal content on the support is the active specie for methane reforming [6].

3.2. Catalytic activity

The catalytic activity of the different catalysts synthesized using α-Al_2O_3, Si_3N_4 and $NiAl_2O_4$ as supports with 10−50% NiO loadings are shown in Figs. 4, 6 and 7. In the case of $NiAl_2O_4$, 0% and 5% NiO results are also included.

Low methane conversions compared to the equilibrium data are obtained with the catalysts that use Si_3N_4 as support. Fig. 4 shows that conversion results in the range of 400 °C−600 °C are far away from the equilibrium values for any of the Ni loadings tested. Conversions close to equilibrium are obtained around 800 °C. Satisfactory results have been also obtained at 800 °C for this catalyst in the methane partial oxidation process [22]. Nevertheless, the optimum temperature reported for operating in SER process is lower than 700 °C [4,7] and, for that reason, in the present work this catalyst support has been discarded. Probably, the low
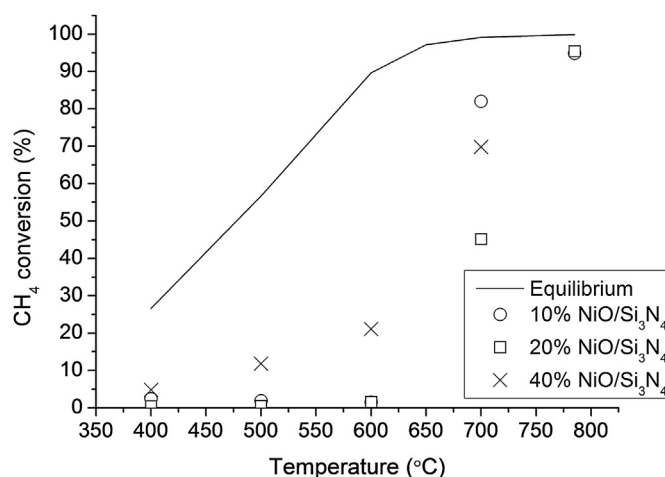

Fig. 4. CH_4 conversion as a function of temperature and Ni loading for NiO/Si_3N_4 catalysts ($S/C \approx 4.4$).

activity could be due to carbon deposition or even may be due to a strong interaction Ni-support. According to SEM-EDX analysis, a high percentage of coke formation (≈ 4 wt.%) is present over Si_3N_4 support although low carbon deposition has been reported previously for its use in the partial oxidation of methane [21]. In fact, the presence of carbon nano-materials has been found by SEM in the 40% NiO/Si_3N_4 sample. Fig. 5 shows carbon filaments deposited over the catalyst surface.

Fig. 6 shows the results obtained for the catalyst $NiO/NiAl_2O_4$. It is observed that conversions close to the equilibrium are obtained for 10% NiO loading. It is also shown that similar results are achieved when NiO loadings higher than 10% are used. However, whilst CH_4 conversions for both 5% $NiO/NiAl_2O_4$ and the stoichiometric spinel structure are lower than the corresponding to the 10% $NiO/NiAl_2O_4$ catalysts from 400 °C to 650 °C, comparable results are obtained at 700 °C and 800 °C. Salhi et al. obtained an increment in methane conversions in SMR when the NiO charges decreased (in
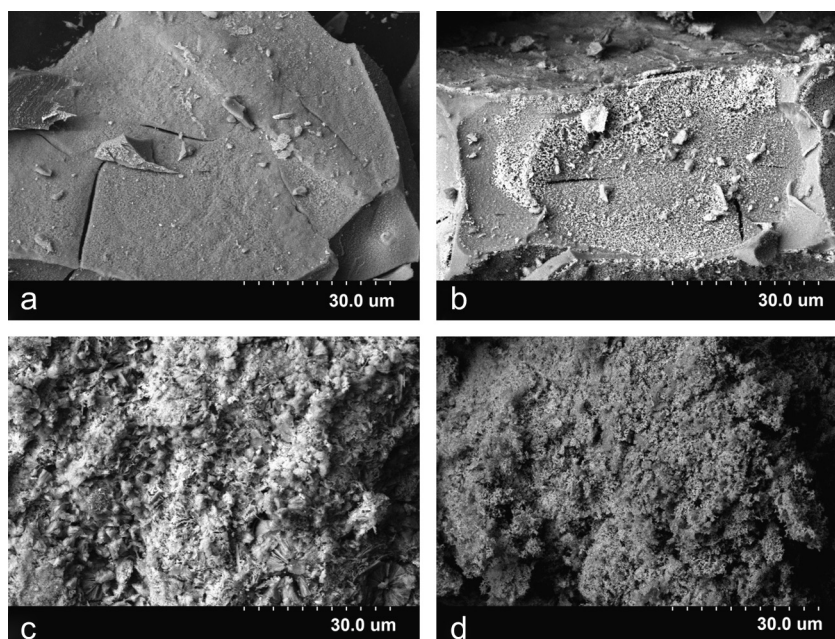

Fig. 3. SEM micrographs of synthesized $NiO/NiAl_2O_4$ catalysts: (a) 0%wt. NiO, (b) 10%wt. NiO, (c) 20%wt. NiO and (d) 50%wt. NiO.

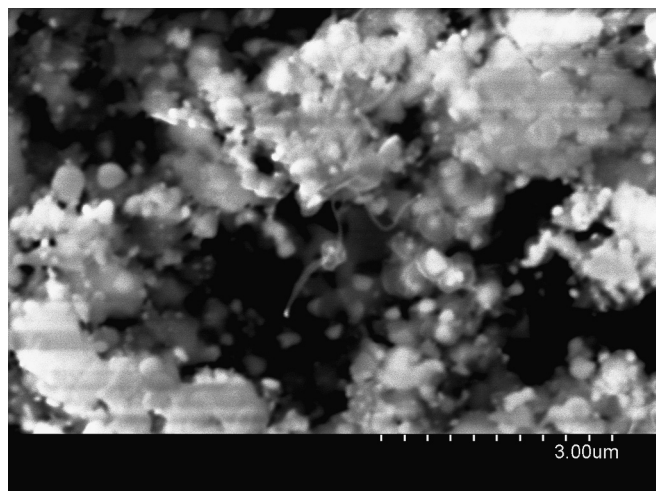**Fig. 5.** SEM micrograph of 40% NiO/Si$_3$N$_4$ catalysts after steam methane reforming.

Fig. 7. CH$_4$ conversion as a function of temperature and Ni loading for NiO/Al$_2$O$_3$ catalysts (S/C ≈ 4.4).

the range of 0–15%, at 500 °C–800 °C and S/C ≈ 3). This trend was attributed by these authors, to the pore blocking when more nickel excess is used [6]. Nevertheless, Sprung et al. [34] reported conversions far to equilibrium in SMR with a 2% NiO/NiAl$_2$O$_4$ at 600 °C and S/C = 0.27–6.3. In SER context, previous works have demonstrated the operability of NiO/NiAl$_2$O$_4$ although with higher Ni loading (60% NiO).

For α-Al$_2$O$_3$ support, it can be observed in Fig. 7, that the best results are obtained for a NiO content of 20%, being this amount comparable to that found in standard commercial catalysts [7]. At low temperatures, low NiO loading (10%) is not enough to attain conversions close to equilibrium. At higher temperatures, conversion results are similar for the 10%–40% NiO loadings and values close to equilibrium are achieved. On the other side, 20% NiO/Al$_2$O$_3$ results are very close to those obtained for the 10% NiO/NiAl$_2$O$_4$. Fig. 8 compares both catalysts in terms of hydrogen yield, showing similar results and all of them close to the equilibrium data.

Problems concerning to deactivation of Ni/α-Al$_2$O$_3$ catalysts due to carbon deposition, are well known [3,12]. However, less carbon deposition is observed from SEM-EDX analysis for the nickel supported Al$_2$O$_3$ catalysts (≈2 wt.%) than for NiO/Si$_3$N$_4$ catalysts.

Carbon nucleation and deposition over Ni catalysts is a very structure sensitive reaction. Thus, smaller particles are more
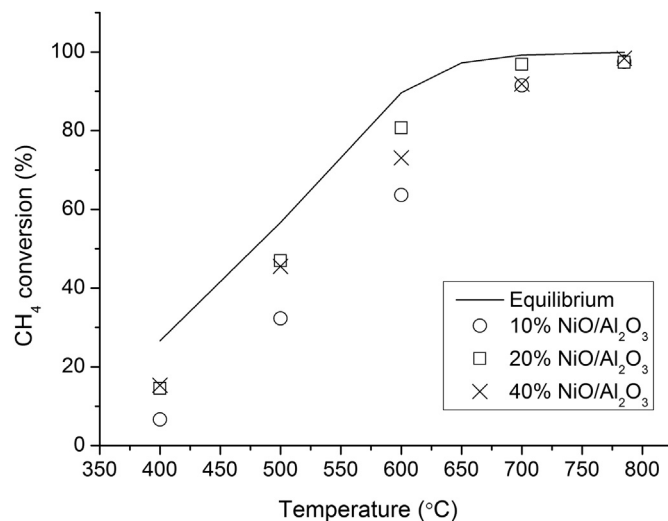
resistant to the initiation of carbon formation [3,33]. However, despite of the bigger NiO crystallite found over NiAl$_2$O$_4$ supports, no relevant carbon amounts have been found by SEM-EDX for 10%– 50% NiO/NiAl$_2$O$_4$, in agreement to the literature data [35]. Thus, it could be assumed that carbon deposition is affected not only by nickel crystallite size but also by the properties of the support [6,36,37]. On the other hand, carbon deposition is detected for lower NiO charges over NiAl$_2$O$_4$ support (0 and 5% NiO), showing a decrease with the nickel loading up to 10 wt.%, when it becomes constant and almost negligible. In summary, the observed trend to carbon deposition on the catalyst surface for study supports is Si$_3$N$_4$ > Al$_2$O$_3$ > NiAl$_2$O$_4$, being negligible the carbon deposition when NiAl$_2$O$_4$ is used as support.

3.3. Catalyst activity after oxidation–reduction cycles

In SER process, the catalyst mixed with the sorbent is proposed to be circulating through the system comprised of the reforming and calcination reactors. The solid mixture remains inside each
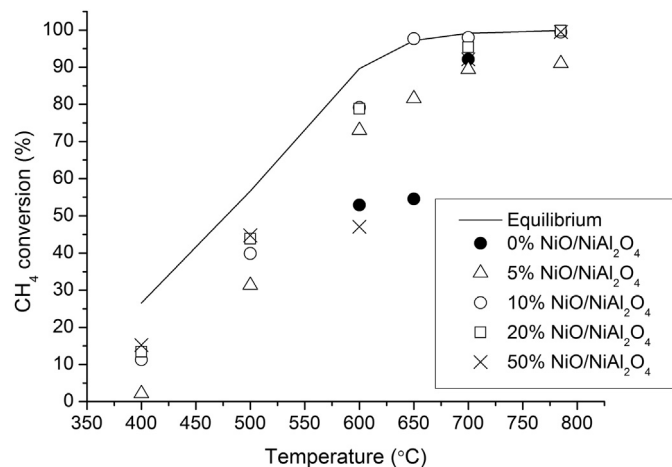

Fig. 6. CH$_4$ conversion as a function of temperature and Ni loading for NiO/NiAl$_2$O$_4$ catalysts (S/C ≈ 4.4).
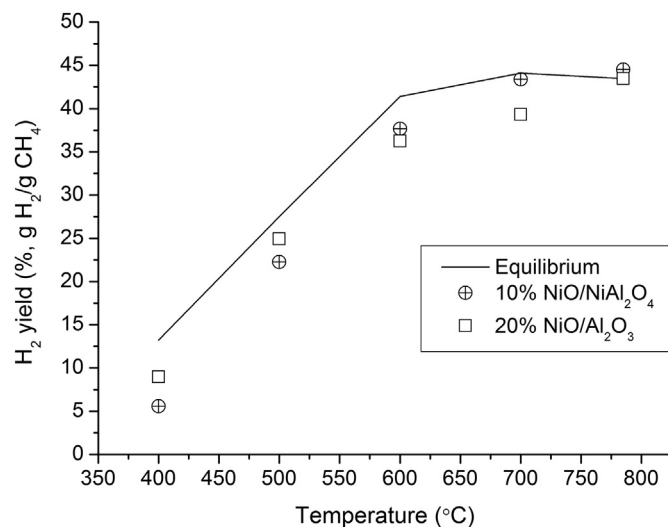

Fig. 8. H$_2$ yield as a function of temperature for 10% NiO/NiAl$_2$O$_4$ and 20% NiO/Al$_2$O$_3$ catalysts (S/C ≈ 4.4).

reactor only for a short period of time, and suffers abrupt changes in the temperature and reaction environment. For this reason, one of the main properties that the selected catalyst must present to work properly in SER process is the capability of maintaining a good reforming activity after oxidation−reduction cycles. Thus, oxidation/reduction cycles have been studied for the two catalysts that showed the best activity (10% $NiO/NiAl_2O_4$ and 20% NiO/Al_2O_3). With this purpose, both samples were cycled in TGA in oxidizing/reducing atmospheres and afterward their activity was measured in the fixed bed micro-reactor under SER typical temperatures.

Methane conversions obtained for the cycled 10% $NiO/NiAl_2O_4$, tested at 600 °C and 650 °C are slightly lower than those obtained for the fresh catalyst, as it is shown in Fig. 9. However, at 700 °C the cycled catalyst still reaches the equilibrium. The reason for this slight deactivation could be an apparent catalyst sintering since no carbon deposition is found according to EDX analysis. Accordingly, the Ni crystallite size change from 68.2 nm for the fresh catalyst to 117.7 nm for the used catalyst and to 154.6 for the cycled used catalyst. The presence of bigger crystallites of NiO on the support surface is also observed by SEM as it is shown in Fig. 10.

The operability of NiO supported over aluminates in SER and sorbent regeneration cycles has been studied in other works, although for higher NiO content (60% $NiO/NiAl_2O_4$) [9,10,25]. High H_2 yields have been reported by different authors operating batchwise during 4 cycles either in a bubbling fluidized bed [9], or in a circulating fluidized bed for 8 h [10]. In both studies, the sorbent has been regenerated with pure N_2. Hildenbrand et al. [25] (operating in switch mode for reforming and calcination, in a bubbling fluidized bed) introduced a variation in the regeneration step by including a 5% O_2 in N_2 to increase the CO_2 evolution rate, obtaining also satisfactory results. In the present work the effect of oxygen in calcination (10% O_2) has been considered of great importance to obtain more reliable conditions and comparable to a potential commercial process, where supplemental fuel should be supplied to give the energy required to release the CO_2 [17]. The good performance of $NiAl_2O_4$ supports for a greater number of reduction/oxidation cycles has been also reported in chemical looping combustion by Johansson et al. [20]. In view of the results obtained and the conclusions presented in the literature, it can be concluded that NiO catalysts supported over $NiAl_2O_4$ could be considered as a perfect candidate to be implemented in SER process at least with respect to its cyclic behavior. It is worth to highlight that the use of a low NiO loading catalyst (10% $NiO/NiAl_2O_4$), compared to usual NiO charges reported in the literature, could be an improvement for the application of this support in SER process.
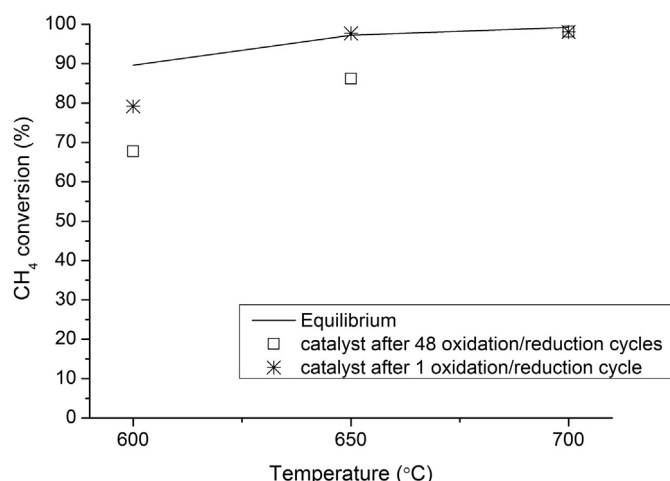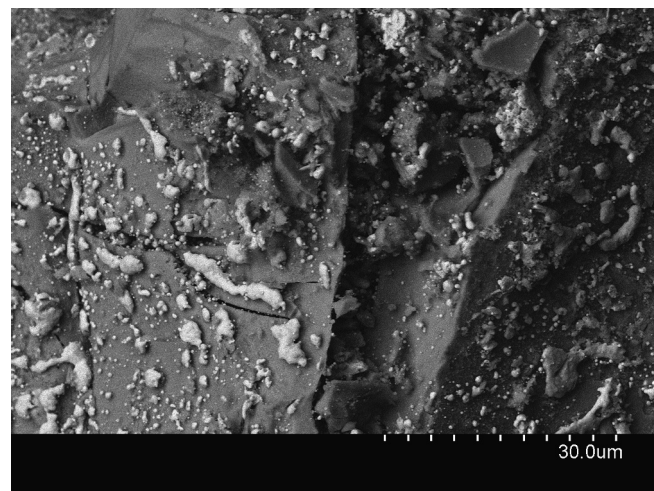

Fig. 10. SEM micrograph of 10% $NiO/NiAl_2O_4$ catalysts after 48 cycles and steam methane reforming.

For the cycled 20% NiO/α-Al_2O_3 catalyst, the catalytic activity decreases respect to the fresh sample at low temperature, from 600 °C to 700 °C. This reduction in the catalytic activity is similar to that observed for 10% $NiO/NiAl_2O_4$. However, both samples show comparable catalytic activity at higher temperature, reaching the equilibrium. The potential use of this catalyst in a cyclic SER process has been studied by Lopez-Ortiz et al. [17], working with 18% NiO/Al_2O_3 in a fixed bed reactor at 650 °C and 15 atm. They reported the production of stable H_2 concentrations near to equilibrium over 5 cycles, using a 4% O_2 in the calcination atmosphere.

According to literature, a possible explanation for the observed activity decrease in α-Al_2O_3 catalysts, could be due to the formation of the spinel phase, $NiAl_2O_4$, in the presence of oxygen at high calcination temperatures and, consequently, the decrease of the available active Ni [31] on the catalyst surface. In the present work, aluminate formation on 20% NiO/α-Al_2O_3 in oxidation−reduction cycles performed in the TGA system described elsewhere [26] has been analyzed by XRD for 1, 25 and 50 oxidation−reduction cycles. Results obtained confirms the aluminate formation over cycles, although appears to be stable after 25 cycles.

Another reason for the activity loss in α-Al_2O_3 catalysts could be the carbon deposition. Nevertheless, results obtained by EDX point out that the formation of coke is not relevant. However, a catalyst sintering has been found by XRD. The Ni crystallite size changes from 49.4 nm for the used catalyst to 85 nm for the cycled catalyst.

A disadvantage reported in the literature for the use of α-Al_2O_3 support in SER is the formation of $Ca_{12}Al_{14}O_{33}$ by interaction of the catalyst and the CaO based sorbent [38] having an adverse effect on the sorbent and catalyst activities. To analyze the possible $Ca_{12}Al_{14}O_{33}$ formation, a mixture comprised of two parts of sorbent (CaO) and one part of catalyst (20% NiO/α-Al_2O_3) was oxidized first for 15 min and later for a longer period of time (4 h). The resulting sample was analyzed by XRD to check the $Ca_{12}Al_{14}O_{33}$ presence. The XRD patterns point out that $Ca_{12}Al_{14}O_{33}$ is not formed either after 15 min or in the sample tested for a longer time.

3.4. Parametric study over 10% $NiO/NiAl_2O_4$ activity

Due to the satisfactory results obtained for 10% $NiO/NiAl_2O_4$ and taking into account the lack of information for the use of low NiO loadings on aluminates supports in SER process, this catalyst has been more extensively studied. First, the steam to methane ratio

Fig. 9. CH_4 conversion for 10% $NiO/NiAl_2O_4$ catalysts after 48 cycles and 1 cycle.

influence on methane conversion and product yields has been analyzed. Additionally, further experiments have been carried out with the purpose of studying the evolution of the activity with both the reaction time and the gas space velocity.

3.4.1. Steam to methane ratio

In SER process, as well as in SMR, it is desirable that catalyst could be able to work at low steam to methane ratios in order to decrease the heat requirements for steam generation at the same time that catalyst activity and hydrogen purity is maintained. In this section, the results obtained for steam to methane ratios in the range of 2.2–4.5 are analyzed.

As expected, methane conversion improves with the S/C ratio. This trend agrees with the results observed in other works where nickel aluminate is also used as support at different NiO contents in SMR [34,35] and in SER [25]. In the present study, methane conversions near to equilibrium are obtained for S/C ratios ranging from 3.3 to 4.5, except at 600 °C for a S/C ratio of 3.3 (see Fig. 11a). However, results obtained at S/C = 2.2 are remarkably lower than the corresponding methane conversion equilibrium data.

Regarding to gas composition, H_2 percentage increases with S/C ratio (Fig. 11b) as a result of the positive effect of H_2O on the reforming and water gas shift reactions. This behavior agrees with Sprung et al. [34], who reported that H_2 percentage increases with steam addition, when CH_4 percentage fed to the system remains constant. In summary, operating at S/C ≈ 3 could be considered a satisfactory result in order to maintain a high catalyst activity
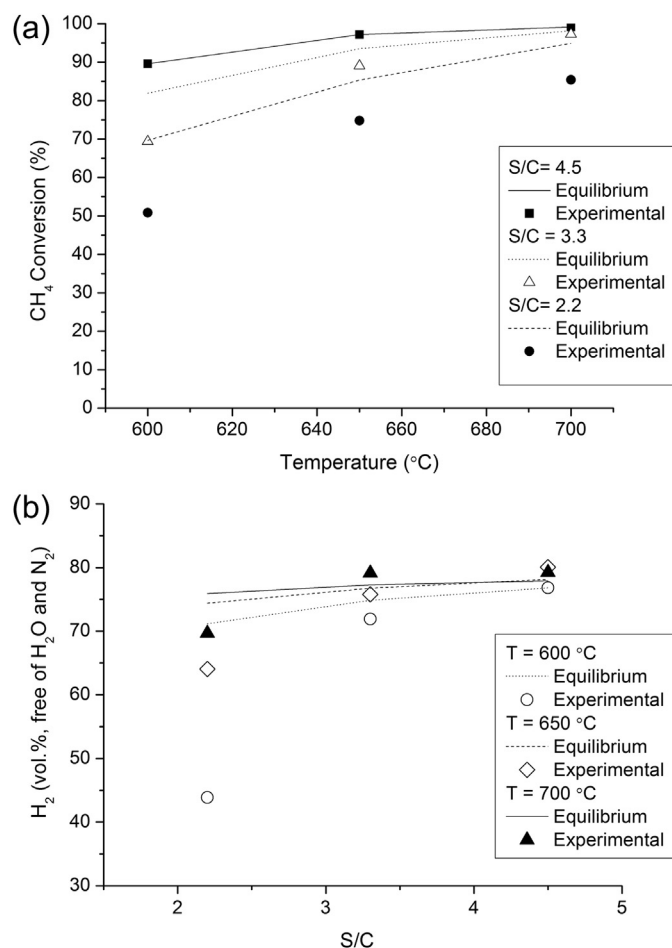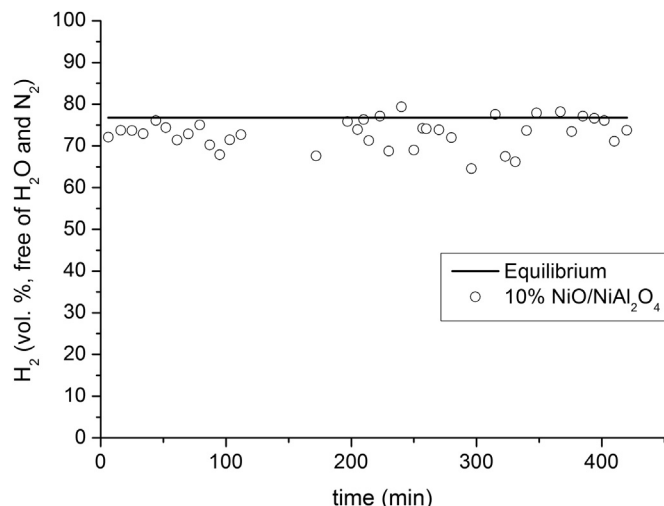

Fig. 12. H_2 gas percentage with time for long duration test with 10% NiO/NiAl$_2$O$_4$ catalyst.

without requiring high energy for steam generation and producing an elevated H_2 concentration. In this sense, it must be taken into account that in SER process, H_2 purity is expected to be improved according to thermodynamic calculations, reaching a 95% for S/C = 3 at 650 °C. It is worth mentioning that although low conversions imposed by the equilibrium restrictions are obtained at low S/C ratios, the comprehensive energy balance could be favorable since the unconverted methane in the reformer could be used as fuel in the calciner (after PSA separation) and lower steam generation is required. Therefore, an S/C ratio as low as 2 could be considered and further analyzed for SER process in future works.

3.4.2. Activity with time for 10% NiO/NiAl$_2$O$_4$ and space velocity influence

A 7 h long experiment is considered enough to demonstrate the stability of this catalyst under reforming conditions, taking into account that in the suggested system for SER process (two interconnected fluidized beds) the average residence time for solids in the reforming reactor is in the order of minutes. A deactivation trend is not appreciated when the catalyst is tested for 7 h continuously at 650 °C and S/C = 3.3. Moreover a hydrogen gas percentage near to equilibrium is still obtained at the end of the experiment as it is shown in Fig. 12. The results obtained agree with
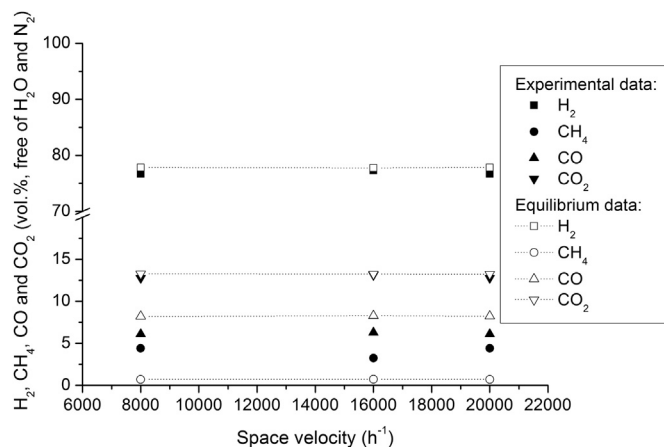

Fig. 11. S/C ratio and temperature influence on 10% NiO/NiAl$_2$O$_4$ catalyst activity (a) CH_4 conversion. (b) H_2 percentage in producer gas.

Fig. 13. Space velocity influence on gas composition.

the stability observed previously by Al-Ubaid and Wolf [35] at similar S/C ratios.

With respect to the space velocity tests, this parameter was varied in the range of 8000 h^{-1}–20,000 h^{-1} for CH$_4$ flow. A good operability with 10% NiO/NiAl$_2$O$_4$ in SMR at these space velocities is an indication of the potential applicability of this catalyst in SER, where less demanding operating conditions are used.

The methane conversion obtained when faster space velocities are used (8000 h^{-1}, 16,000 h^{-1} and 20,000 h^{-1} for CH$_4$ flow) at 650 °C is higher than 80%, with a H$_2$ concentration in producer gas around 76–78% vol. (dry basis). Therefore, it can be concluded that no significant change on gas composition with space velocity could be observed (Fig. 13).

4. Conclusions

Si$_3$N$_4$, α-Al$_2$O$_3$ and NiAl$_2$O$_4$ supported nickel catalysts have been synthesized and tested in a fixed bed micro-reactor to analyze their behavior at low temperature conditions and multiple reduction–oxidation cycles in order to be used as reforming catalyst in a SER process. Catalysts with different NiO loading have been prepared and characterized following diverse routes and by using diverse analytical techniques.

The obtained results show that, regardless the NiO loading, NiO/Si$_3$N$_4$ catalyst is not appropriate to work under typical SER conditions since low conversions far from the equilibrium are obtained at the usual process temperature.

A good performance has been observed for nickel supported Al$_2$O$_3$ and NiAl$_2$O$_4$ catalysts at low temperatures. The highest methane conversion, close to equilibrium at 600 °C–700 °C and S/C = 4.5, has been obtained for 10% NiO/NiAl$_2$O$_4$ and 20% NiO/Al$_2$O$_3$. No significant influence is found for the NiO loading in the case of the NiAl$_2$O$_4$ support, from 10% NiO to 50% NiO. In the case of Al$_2$O$_3$ support, no considerable influence is detected for the NiO loading at temperatures higher than 700 °C but this influence is remarkable at lower temperatures for 10% NiO to 40% NiO loadings.

No relevant carbon deposition has been found in used NiO/NiAl$_2$O$_4$ catalysts. The observed trend of the carbon deposition for the studied supports is Si$_3$N$_4$ > Al$_2$O$_3$ > NiAl$_2$O$_4$.

10% NiO/NiAl$_2$O$_4$ and 20% NiO/Al$_2$O$_3$ show enough catalytic activity after oxidation/reduction cycles in spite of the sintering observed for NiAl$_2$O$_4$ catalyst or the formation of NiAl$_2$O$_4$ in Al$_2$O$_3$ catalyst.

Regarding to steam/methane ratio, catalytic activity of 10% NiO/NiAl$_2$O$_4$ in the range of 600 °C–700 °C and S/C = 3.3 is very close to equilibrium. In the range of 600 °C–700 °C and S/C = 2.2, methane conversion is lower than equilibrium data.

Acknowledgments

Appendix A. Supporting information

Supplementary data related to this article can be found online at http://dx.doi.org/10.1016/j.jpowsour.2013.05.069.

References

[1] M. Balat, Int. J. Hydrogen Energy 33 (2008) 4013–4029.
[2] A. Konieczny, K. Mondal, T. Wiltowski, P. Dydo, Int. J. Hydrogen Energy 33 (2008) 264–272.
[3] J.R. Rostrup-Nielsen, J. Sehested, Adv. Catal. 47 (2002) 65–139.
[4] D.P. Harrison, Ind. Eng. Chem. Res. 47 (2008) 6486–6501.
[5] A.P. Simpson, A.E. Lutz, Int. J. Hydrogen Energy 32 (2007) 4811–4820.
[6] N. Salhi, A. Boulahouche, C. Petit, A. Kiennemann, C. Rabia, Int. J. Hydrogen Energy 36 (2011) 11433–11439.
[7] B. Balasubramanian, A. Lopez Ortiz, S. Kaytakoglu, D.P. Harrison, Chem. Eng. Sci. 54 (1999) 3543–3552.
[8] K. Johnsen, J.R. Grace, S.S.E. H Elnashaie, L. Kolbeinsen, D. Eriksen, Ind. Eng. Chem. Res. (2006) 4133–4144.
[9] K. Johnsen, H.J. Ryu, J.R. Grace, C.J. Lim, Chem. Eng. Sci. 61 (2006) 1195–1202.
[10] B. Arstad, J. Prostak, R. Blom, Chem. Eng. J. 189–190 (2012) 413–421.
[11] E. Ochoa Fernandez, G. Haugen, T. Zhao, M. Ronning, I. Aartum, B. Borresen, E. Rytter, M. Ronnekleiv, D. Chen, Green Chem. 9 (2007) 654–662.
[12] H.E. Roh, K.W. Jun, S.E. Park, Hyun-Seog Roh, Ki-Won Jun, Sang-Eon Park, Appl. Catal. A Gen. 251 (2003) 275–283.
[13] A.I. La Cava, C.A. Bernardo, D.L. Trimm, Carbon 20 (1982) 219–223.
[14] J.R. Rostrup-Nielsen, J. Catal. 85 (1984) 31–43.
[15] J.R. Rostrup-Nielsen, J. Catal. 48 (1977) 155–165.
[16] C.H. Bartholomew, Appl. Catal. A Gen. 212 (2001) 17–60.
[17] A. Lopez Ortiz, D.P. Harrison, Ind. Eng. Chem. Res. 40 (2001) 5102–5109.
[18] K.B. Yi, D.P. Harrison, Ind. Eng. Chem. Res. 44 (2005) 1665–1669.
[19] Z.-S. Li, N.-S. Cai, Energy Fuel 21 (2007) 2909–2918.
[20] M. Johansson, T. Mattisson, A. Lyngfelt, Ind. Eng. Chem. Res. 45 (2006) 5911–5919.
[21] R. Shang, X. Guo, S. Mu, Y. Wang, G. Jin, H. Kosslick, A. Schulz, X.-Y. Guo, Int. J. Hydrogen Energy 36 (2011) 4900–4907.
[22] R. Shang, W. Sun, Y. Wang, G.-Q. Jin, X.-Y. Gou, Catal. Comun. 9 (2008) 2103–2106.
[23] N.F.P. Ribeiro, R.C.R. Neto, S.F. Moya, A.M.V.M. Souza, M. Schmal, Int. J. Hydrogen Energy 35 (2010) 11725–11732.
[24] J.E. Readman, A. Olafsen, J.B. Smith, R. Blom, Energy Fuel 20 (2006) 1382–1387.
[25] N. Hildenbrand, J. Readman, I.M. Dahl, R. Blom, Appl. Catal. A Gen. 303 (2006) 131–137.
[26] A.L. Garcia-Lario, I. Martínez, R. Murillo, G.S. Grasa, J.R. Fernandez, J.C. Abanades, Ind. Eng. Chem. Res. http://dx.doi.org/10.1021/ie3012598.
[27] F. Pompeo, N.N. Nichio, O.A. Ferretti, D. Resasco, Int. J. Hydrogen Energy 30 (2005) 1399–1405.
[28] O. Levenspiel, Chemical Reaction Engineering, third sub ed., Wiley, August 13, 1998, pp. 298–319.
[29] K. Hou, R. Hughes, Chem. Eng. J. 82 (2001) 311–328.
[30] G.R. Gavalas, C. Phichitkul, G.E. Voecks, J. Catal. 88 (1984) 54–64.
[31] T. Numaguchi, K. Kikuchi, Ind. Eng. Chem. Res. 30 (1991) 447–453.
[32] P.H. Bolt, S.F. Lobner, T.P. Van den Bout, J.W. Geus, F.H.P.M. Habraken, Appl. Surf. Sci. 70/71 (1993) 196–199.
[33] K.O. Christensen, D. Chen, R. Lødeng, A. Holmen, Appl. Catal. A Gen. 314 (2006) 9–22.
[34] C. Sprung, B. Arstad, U. Olsbye, Top Catal. 54 (2011) 1063–1069.
[35] A. Al-Ubaid, E. Wolf, Appl. Catal. 40 (1988) 73–85.
[36] T. Borowiecki, Appl. Catal. 10 (1984) 273–289.
[37] S. Wang, G.Q.M. Lu, Appl. Catal. B Environ. 16 (1998) 269–277.
[38] M.E. Agnelli, M.C. Micheli, E.N. Ponzi, Ind. Eng. Chem. Res. 26 (1987) 1707–1713.